Abbreviated Terms

The following abbreviations are used throughout this chapter:

Abbreviation	**Full Term**
CPO	Co-Packaged Optics
CMT	Coupled Mode Theory
DEE	Differentiable Eikonal Engine
EIC	Electronic Integrated Circuit
FOM	Figure of Merit
FSR	Free Spectral Range
HOM	Hong-Ou-Mandel
PIC	Photonic Integrated Circuit
QFI	Quantum Fisher Information
WDM	Wavelength Division Multiplexing

Table 5.1: Chapter 5 Notation Summary

Symbol	**Meaning**	**Units/Range**
$a_j(z)$	Mode amplitude in waveguide j	[complex, arb.]
β_j	Propagation constant	[rad/mm]
κ_{jk}	Coupling coefficient	[mm^{-1}]
$\mathbf{C}$	Coupling matrix	$N \times N$
$\mathbf{V}$	Eigenvector matrix	$N \times N$
β_k	Eigenvalue (supermode)	[rad/mm]
$\Delta\beta$	Eigenvalue spacing	[rad/mm]
L	Device length	[mm]
p	Waveguide pitch	[μm]
η	Coupling efficiency	[0, 1]
$\bar{\eta}$	Mean coupling efficiency	[0, 1]
U	Uniformity $= \eta_{\min}/\eta_{\max}$	[0, 1]
X_{jk}	Crosstalk from j to k	[dB]
$\mathcal{F}$	Quantum gate fidelity	[0, 1]
V_{HOM}	HOM visibility	[0, 1]
λ	Wavelength	[nm]
$\Delta\lambda$	Channel spacing (WDM)	[nm]
D_{eff}	Effective dimensionality	[–]
$\kappa(\mathbf{V})$	Condition number	≥ 1

Chapter 5
Photonic Integration

Learning Objectives

After completing this chapter, you will be able to:

1. Classify photonic integration problems by **effective dimensionality** (0-D to quasi-3D)
2. Identify **non-uniformity** as the universal pain point and quantify its impact at each dimension
3. Understand WDM as a **dimensional multiplier** that transforms spatial problems
4. Derive coupled mode equations and recognize eigenvalues β_k as eikonals
5. Apply the **Walther-Matsui-Nariai duality** to multi-dimensional coupler design
6. Implement DEE-Waveguide in JAX with automatic differentiation
7. Analyze scaling laws: eigenvalue crowding as N increases
8. Design for **orthogonality preservation** across dimensions
9. Connect classical waveguide arrays to quantum walks and photonic gates
10. Translate classical specifications to quantum requirements with proper tolerance analysis

5.1 Introduction and Pain Points

Photonic integration represents the transition from discrete optical components to monolithic waveguide circuits—analogous to the transition from vacuum tubes to integrated circuits in electronics. Modern data centers, quantum computers, and sensing systems increasingly rely on photonic integrated circuits (PICs) that combine dozens to hundreds of waveguides on a single chip.

This chapter establishes a computational framework for designing such integrated photonic systems using the eigenmode–eikonal formalism. The central insight is simple but powerful: the eigenvalues of the coupling matrix are the eikonals for the coupled system. In other words, the same quantity that measures phase accumulation in Part I reappears here as the spectrum that governs how power and information propagate through a coupled waveguide network.

Before we write down the coupled-mode equations, it helps to name the engineering difficulty that makes photonic integration feel "hard" in practice. The difficulty is not that any one axis is unfamiliar. It is that real systems must satisfy multiple axes *at the same time*—and the failure of just one axis often destroys the assumptions that make the others analyzable.

Pain Points: The Multi-Dimensional Challenge

The fundamental challenge of photonic integration is **multi-dimensional**: systems must work across spatial channels (scaling), spectral channels (WDM), and fabrication variations (non-uniformity)—simultaneously.

The statement above is deliberately general; the next box compresses it into a single "production equation." Read it as a reminder that scaling, WDM, and fabrication variation are not three separate projects—they are three coupled dimensions of the *same* design space.

Pain Points: Scaling × WDM × Non-uniformity

Every real system faces this three-way challenge:

$$\textbf{Scaling} \times \textbf{WDM} \times \textbf{Non-uniformity} = \textbf{Production Reality}$$

When any of these factors causes **eigenmode orthogonality to break**, crosstalk emerges and performance degrades. The eigenmode-eikonal framework provides the unified diagnostic and design methodology.

Once you accept this as the production reality, two concrete questions show up immediately, and they are the same two questions that have organized this book from the beginning:

1. **Forward analysis (Walther):** given a specific geometry (hence a specific coupling matrix), what does the device do across channels, wavelengths, and expected variation?

2. **Inverse design (Matsui–Nariai):** given a target specification across those same dimensions, what physical parameters and fabrication tolerances are required to make it work?

The next two boxes state these questions in the form engineers actually use: the first is a prediction task (compute worst-case behavior without brute-force enumeration), and the second is a synthesis task (choose geometry and tolerance budgets that guarantee performance). Keep them in mind—most of the chapter is just different ways of making these two questions computable, fast, and diagnosable.

WALTHER (Forward Analysis)

Pain Point: "Given coupling coefficients κ and device length L, what is the output power distribution $P(z)$? How does it vary across 64 spatial channels AND 40 WDM wavelengths when fabrication introduces $\pm 5\%$ coupling variation?"
Situation: You have a co-packaged optics (CPO) module with known geometry and need to predict worst-case channel performance.
Challenge: The problem has $64 \times 40 = 2560$ channel-wavelength combinations, each affected by non-uniformity. Direct evaluation is prohibitive.
Solution Preview: Eigendecomposition plus sensitivity analysis via JAX autodiff identifies the critical failure modes without exhaustive enumeration.

MATSUI-NARIAI (Inverse Design)

Pain Point: "I need coupling efficiency $> 90\%$ with uniformity $> 95\%$ across all channels and wavelengths. What design parameters achieve this? How tight must fabrication tolerances be?"
Situation: You have target specifications spanning multiple dimensions and need to determine physical design parameters plus manufacturing requirements.
Challenge: The design space is high-dimensional: waveguide geometry, pitch, length, plus robustness to non-uniformity.
Solution Preview: The Matsui-Nariai inverse framework with Hessian-based tolerance analysis determines both optimal design AND required fabrication precision.

Together, these three boxes set the agenda for Chapter 5: we will (i) quantify how orthogonality fails as dimensionality grows, (ii) use eigenmodes to reduce complexity while preserving physics, and (iii) make both the forward and inverse workflows differentiable so that sensitivity and tolerance analysis become first-class outputs rather than afterthoughts.

The chapter proceeds as follows: Section 5.2 explains why eigenmode analysis leads Part II. Section 5.3 introduces the dimensional hierarchy that organizes all photonic integration challenges. Sections 5.4–5.6 develop the mathematical framework. Section 5.7 presents the JAX implementation. Section 5.8 provides a comprehensive practical example progressing from 0-D to quasi-2D. Section 5.9 establishes the quantum connection. Section 5.10 identifies failure modes.

5.2 Why Eigenmode and Orthogonality Lead Part II

Part II of this book covers computational optics: the algorithms and methods that transform optical design from art to engineering. Why does eigenmode analysis appear first, before optimization (Chapter 6), the full DEE framework (Chapter 7), or the unified Walther-Matsui-Nariai duality (Chapter 8)?

5.2.1 The Computational Foundation

Eigendecomposition is the computational primitive upon which all subsequent chapters build:

1. **Complexity reduction:** Eigendecomposition transforms $O(N^3)$ per-step operations into $O(N^3)$ once plus $O(N^2)$ per-step, enabling the massive iteration counts required for optimization.

2. **Gradient access:** JAX can differentiate through eigendecomposition, providing $\partial\beta_k/\partial p$ for any design parameter p. This is the foundation of Chapter 7's DEE.

3. **Physical insight:** Eigenvalues are not abstract numbers—they are the eikonals (optical path rates) for the coupled system. This connects Part II directly to Part I.

5.2.2 Orthogonality: The Universal Requirement

Every performance metric in photonic integration ultimately traces to eigenmode orthogonality:

Table 5.2: Orthogonality Connection to Performance Metrics

Metric	Orthogonality Condition	Failure Mode
Crosstalk X_{jk}	$\langle\psi_j\|\psi_k\rangle = \delta_{jk}$	Mode mixing
Uniformity U	Equal eigenvalue spacing	Edge effects
Bandwidth	$\partial\beta_k/\partial\lambda$ uniform	Dispersion
Fidelity $\mathcal{F}$	Unitary evolution preserved	Decoherence

Key Insight

The Central Thesis of Chapter 5: Every challenge in photonic integration—scaling, WDM, non-uniformity, coupling geometry—can be traced to eigenmode orthogonality. When orthogonality is preserved, systems work. When it breaks, they fail. The eigenmode-eikonal framework provides the tools to diagnose, predict, and design for orthogonality preservation.

5.2.3 The Eigenvalue-Eikonal Identity

The most important equation in this chapter connects eigenvalues to eikonals:

$$\boxed{\beta_k = \frac{dW_k}{dz} \cdot \frac{2\pi}{\lambda}} \tag{5.1}$$

This identity states that each eigenvalue β_k is exactly the rate of phase accumulation for eigenmode k—the guided-wave analog of the eikonal equation from ray optics. The implications cascade through Part II:

- **Chapter 6:** The eigenvalue spectrum determines the energy landscape for optimization
- **Chapter 7:** JAX autodiff through eigendecomposition enables the DEE
- **Chapter 8:** Both Walther and Matsui-Nariai paths share eigendecomposition as their core

5.3 The Dimensional Hierarchy of Photonic Integration

Real photonic systems operate across multiple dimensions simultaneously. This section introduces the dimensional hierarchy that organizes all integration challenges and reveals WDM as a "dimensional multiplier."

5.3.1 From 0-D to Quasi-3D: A Unified View

Photonic coupling problems can be classified by their effective dimensionality:

Table 5.3: Dimensional Hierarchy of Photonic Integration

Dimension	Configuration	Coupling Matrix	Key Challenge	FOM
0-D	Single channel	Scalar κ	Mode matching	η
Quasi-1D	0-D + WDM	$\kappa(\lambda)$	Dispersion	$\eta(\lambda)$, BW
1-D	Linear array	$\mathbf{C}_{N\times N}$	Eigenvalue crowding	U, X_{jk}
Quasi-2D	1-D + WDM	$\mathbf{C}(\lambda)$	Joint degradation	$U(\lambda)$
2-D	Fiber bundle	$\mathbf{C}_{N\times M}$	Registration, tilt	η_{jk} matrix
Quasi-3D	2-D + WDM	$\mathbf{C}(\lambda)_{N\times M}$	All combined	Tensor $\eta_{jk}(\lambda)$

The effective dimensionality D_{eff} determines computational complexity and design difficulty:

$$D_{\text{eff}} = D_{\text{spatial}} + D_{\text{spectral}} + D_{\text{variation}} \tag{5.2}$$

where $D_{\text{spectral}} = 1$ when WDM is included (0 otherwise) and $D_{\text{variation}}$ captures the degrees of freedom in non-uniformity.

5.3.2 WDM as Dimensional Multiplier

Wavelength Division Multiplexing (WDM) is not merely a technique for increasing bandwidth—it fundamentally transforms the design space by adding a spectral dimension to every spatial problem.

Dimensional Analysis

WDM Multiplier Effect:

- 0-D $\rightarrow$ Quasi-1D: Single coupler becomes wavelength-dependent $\kappa(\lambda)$
- 1-D array $\rightarrow$ Quasi-2D: N channels become $N \times M$ channel-wavelength combinations
- Performance degrades at "corners" of the channel-wavelength space

The coupling coefficient's wavelength dependence is:

$$\kappa(\lambda) = \kappa_0 \exp\left(-\frac{g}{\lambda_{\text{decay}}}\right) \cdot \left(1 + \alpha_\lambda \frac{\lambda - \lambda_0}{\lambda_0}\right) \tag{5.3}$$

where α_λ captures dispersion. For silicon photonics, typically $|\alpha_\lambda| \approx 0.1$–$0.3$.

5.3.3 Non-uniformity at Each Dimension

Fabrication variations introduce non-uniformity that compounds with dimensionality:

Non-uniformity Alert

Non-uniformity Scaling Law:
For $\delta\kappa/\kappa$ coupling variation, the performance degradation scales as:

$$\Delta\eta \propto \left(\frac{\delta\kappa}{\kappa}\right)^2 \cdot N^\gamma \tag{5.4}$$

where $\gamma \approx 1$ for 1-D arrays and $\gamma \approx 2$ for 2-D arrays. The quadratic dependence on non-uniformity explains why "5% variation" often produces "25% performance loss."
Mitigation: Add "dummy" waveguides at boundaries that are not used for signal but provide symmetric coupling environment.

5.3.4 Orthogonality Preservation Requirements

At each dimensional level, orthogonality preservation requires maintaining eigenvalue spacing:

$$\Delta\beta_{\min} > \gamma_{\text{threshold}} \tag{5.5}$$

where $\gamma_{\text{threshold}}$ depends on the application:

Table 5.4: Eigenvalue Spacing Requirements

Application	$\Delta\beta_{\min}$ **Requirement**	**Rationale**
Classical telecom	$> \alpha_{\text{loss}}$ (0.01 mm^{-1})	Mode distinguishable before loss
High-density CPO	$> 10 \times \delta\beta_{\text{fab}}$	Fabrication tolerance margin
Quantum gates	$> 100 \times \delta\beta_{\text{fab}}$	Fidelity $> 99.9\%$

The effective spacing must be maintained across *all* dimensions:

$$\Delta\beta_{\text{eff}} = \min\left\{\Delta\beta_{\text{spatial}}(N), \Delta\beta_{\text{spectral}}(\lambda), \Delta\beta_{\text{fab}}(\delta p)\right\} \tag{5.6}$$

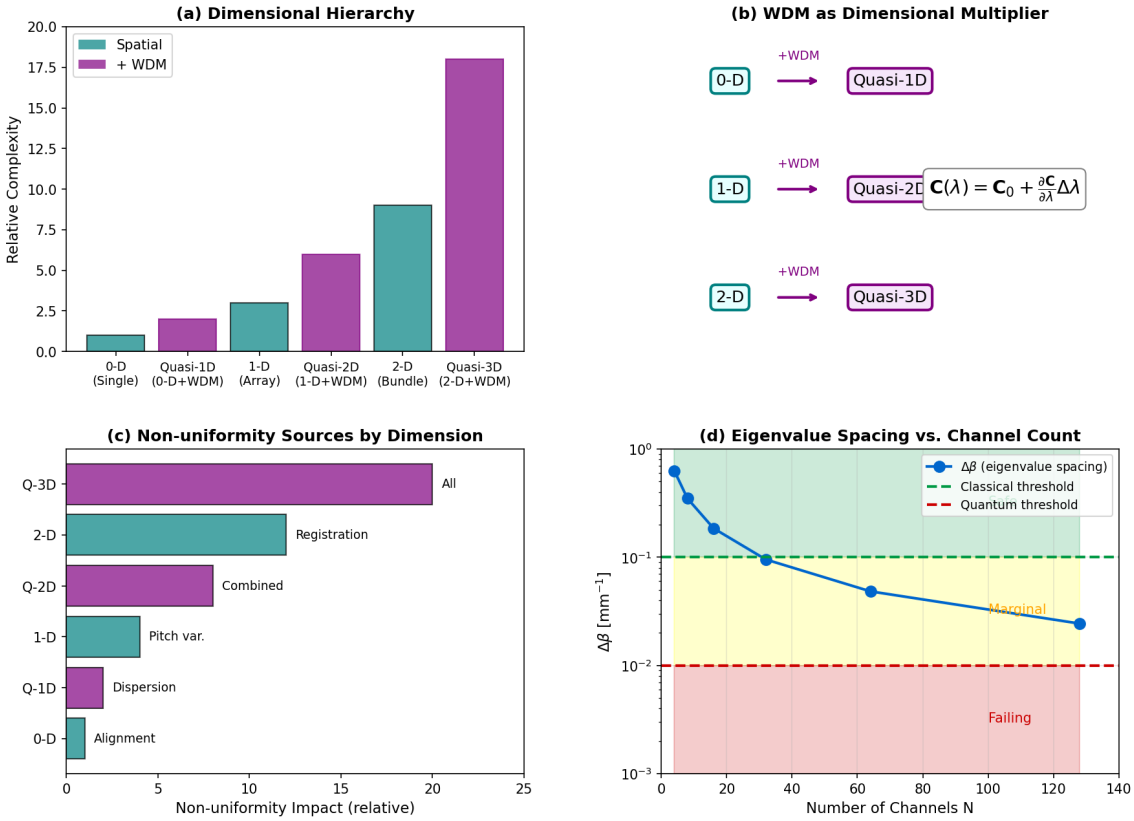

Figure 5.1: Dimensional hierarchy of photonic integration. (a) Progression from 0-D single channel to quasi-3D (2D array + WDM). (b) WDM as dimensional multiplier: each spatial configuration gains an additional spectral axis. (c) Non-uniformity impact at each level. (d) Eigenvalue spacing $\Delta\beta$ requirements for orthogonality preservation.

5.4 Coupled Mode Theory Fundamentals

5.4.1 The Waveguide Array Problem

Consider N single-mode waveguides arranged in parallel, each supporting a fundamental mode with propagation constant β_j. When the waveguides are sufficiently close, evanescent field overlap leads to optical coupling. The electric field in waveguide j can be written as:

$$E_j(x, y, z, t) = a_j(z) \cdot e_j(x, y) \cdot \exp(i\beta_j z - i\omega t) \tag{5.7}$$

where $a_j(z)$ is the slowly varying complex amplitude, $e_j(x, y)$ is the transverse mode profile, and β_j is the isolated-waveguide propagation constant.

The coupled mode equations govern the evolution of mode amplitudes:

$$\frac{da_j}{dz} = -i\beta_j a_j - i\sum_{k\neq j} \kappa_{jk} a_k \tag{5.8}$$

In matrix form:

$$\frac{d\mathbf{a}}{dz} = -i\mathbf{C}\mathbf{a} \tag{5.9}$$

where the coupling matrix $\mathbf{C}$ has elements:

$$C_{jk} = \begin{cases} \beta_j & j = k \\ \kappa_{jk} & j \neq k \end{cases} \tag{5.10}$$

5.4.2 Coupling Coefficients and Non-uniformity

The coupling coefficient between waveguides j and k arises from mode overlap:

$$\kappa_{jk} = \frac{\omega \varepsilon_0}{4} \iint \Delta n_{jk}^2(x,y) \cdot e_j^*(x,y) \cdot e_k(x,y)\, dx\, dy \tag{5.11}$$

where Δn_{jk}^2 represents the refractive index perturbation that waveguide k creates in the region of waveguide j.

For identical waveguides with uniform spacing, nearest-neighbor coupling dominates:

$$\kappa_{jk} \approx \kappa_0 \exp(-\gamma |j-k| d) \tag{5.12}$$

where κ_0 is the nearest-neighbor coupling strength, γ is the decay constant (typically 1–3 μm^{-1} for silicon photonics), and d is the waveguide pitch.

Non-uniformity Alert

Non-uniformity in Coupling: Real systems deviate from the ideal:

$$\kappa_{jk}^{\text{real}} = \kappa_{jk}^{\text{ideal}}(1 + \delta_{jk}) \tag{5.13}$$

Sources of δ_{jk}:

- **Systematic:** Lithography gradient across die ($\delta \sim 0.01$–0.05)
- **Random:** Line edge roughness ($\delta \sim 0.001$–0.01)
- **Edge effects:** Boundary waveguides see asymmetric environment

Impact: Non-uniform coupling breaks the translational symmetry of $\mathbf{C}$, causing eigenvector rotation and orthogonality degradation.

5.4.3 The Coupling Matrix: From Ideal to Real

The ideal coupling matrix for a uniform array with nearest-neighbor coupling is tridiagonal:

$$\mathbf{C}_{\text{ideal}} = \begin{pmatrix} \beta_0 & \kappa & 0 & \cdots & 0 \\ \kappa & \beta_0 & \kappa & \cdots & 0 \\ 0 & \kappa & \beta_0 & \ddots & \vdots \\ \vdots & \ddots & \ddots & \ddots & \kappa \\ 0 & \cdots & 0 & \kappa & \beta_0 \end{pmatrix} \tag{5.14}$$

The real coupling matrix includes perturbations:

$$\mathbf{C}_{\text{real}} = \mathbf{C}_{\text{ideal}} + \delta\mathbf{C} \tag{5.15}$$

where $\delta\mathbf{C}$ captures fabrication variations, thermal gradients, and edge effects.

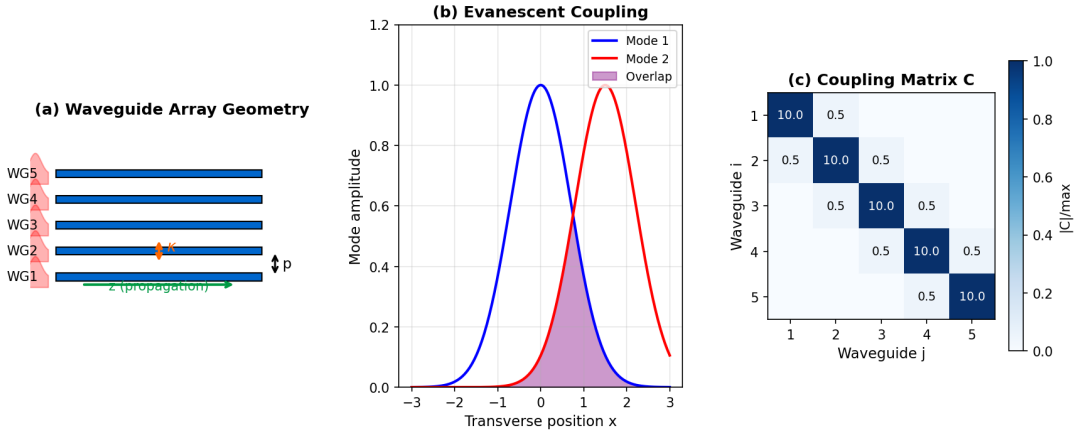

Figure 5.2: Coupled waveguide array geometry. (a) N waveguides with pitch p and nearest-neighbor coupling κ. (b) Mode profiles showing evanescent overlap in coupling region. (c) Ideal vs. real coupling matrix structure, showing how non-uniformity breaks tridiagonal symmetry.

5.5 Matrix Exponential and Eigendecomposition

5.5.1 Formal Solution

The coupled mode equation (5.9) has the formal solution:

$$\mathbf{a}(z) = \exp(-i\mathbf{C}z) \cdot \mathbf{a}(0) \tag{5.16}$$

Direct evaluation of the matrix exponential requires computing:

$$\exp(-i\mathbf{C}z) = \sum_{n=0}^{\infty} \frac{(-i\mathbf{C}z)^n}{n!} \tag{5.17}$$

which costs $O(N^3)$ operations per propagation point using Padé approximation or scaling-and-squaring.

5.5.2 Eigendecomposition Solution

The coupling matrix admits eigendecomposition:

$$\mathbf{C} = \mathbf{V}\mathbf{D}\mathbf{V}^{-1} \tag{5.18}$$

where $\mathbf{D} = \text{diag}(\beta_1, \beta_2, \ldots, \beta_N)$ contains eigenvalues and $\mathbf{V}$ contains eigenvectors as columns.

The matrix exponential simplifies dramatically:

$$\exp(-i\mathbf{C}z) = \mathbf{V} \cdot \text{diag}(e^{-i\beta_1 z}, \ldots, e^{-i\beta_N z}) \cdot \mathbf{V}^{-1} \tag{5.19}$$

The algorithm proceeds in three steps:

1. **Transform to eigenmode basis:** $\mathbf{b}(0) = \mathbf{V}^{-1}\mathbf{a}(0)$

2. **Propagate each eigenmode:** $b_k(z) = b_k(0)\exp(-i\beta_k z)$
3. **Transform back:** $\mathbf{a}(z) = \mathbf{V}\mathbf{b}(z)$

5.5.3 Computational Complexity

Table 5.5: Computational Complexity Comparison

Method	**Setup**	**Per-z point**	**Total (M points)**
Direct $\exp(-i\mathbf{C}z)$	—	$O(N^3)$	$O(MN^3)$
Eigendecomposition	$O(N^3)$	$O(N^2)$	$O(N^3 + MN^2)$
Speedup factor	—	—	$\mathbf{M/(1+M/N)}$

For typical CPO design with $N = 32$ waveguides and $M = 1000$ optimization iterations, this yields a theoretical speedup of $\approx 31\times$. With JAX GPU acceleration, observed speedups exceed $500\times$.

5.5.4 Non-uniform Coupling: Breaking Symmetry

For the ideal tridiagonal matrix, eigenvalues have analytical form:

$$\beta_k^{\text{ideal}} = \beta_0 + 2\kappa\cos\left(\frac{k\pi}{N+1}\right), \quad k = 1, 2, \ldots, N \tag{5.20}$$

with spacing:

$$\Delta\beta \approx \frac{2\pi\kappa}{N+1} \sim \frac{1}{N} \tag{5.21}$$

Key Insight

Eigenvalue Crowding: As array size N increases, eigenvalue spacing $\Delta\beta$ decreases as $1/N$. This is the fundamental scaling limit: modes become increasingly difficult to distinguish, orthogonality degrades, and crosstalk rises.

Non-uniformity perturbs both eigenvalues and eigenvectors:

$$\beta_k^{\text{real}} = \beta_k^{\text{ideal}} + \delta\beta_k, \quad \mathbf{v}_k^{\text{real}} = \mathbf{v}_k^{\text{ideal}} + \delta\mathbf{v}_k \tag{5.22}$$

The eigenvector perturbation causes mode mixing and crosstalk:

$$X_{jk} = \left|\langle\mathbf{v}_j^{\text{real}}|\mathbf{v}_k^{\text{ideal}}\rangle\right|^2 \approx \left|\frac{\langle\mathbf{v}_j|\delta\mathbf{C}|\mathbf{v}_k\rangle}{\beta_j - \beta_k}\right|^2 \tag{5.23}$$

Note the $1/(\beta_j - \beta_k)^2$ dependence: crosstalk is amplified when eigenvalues are nearly degenerate.

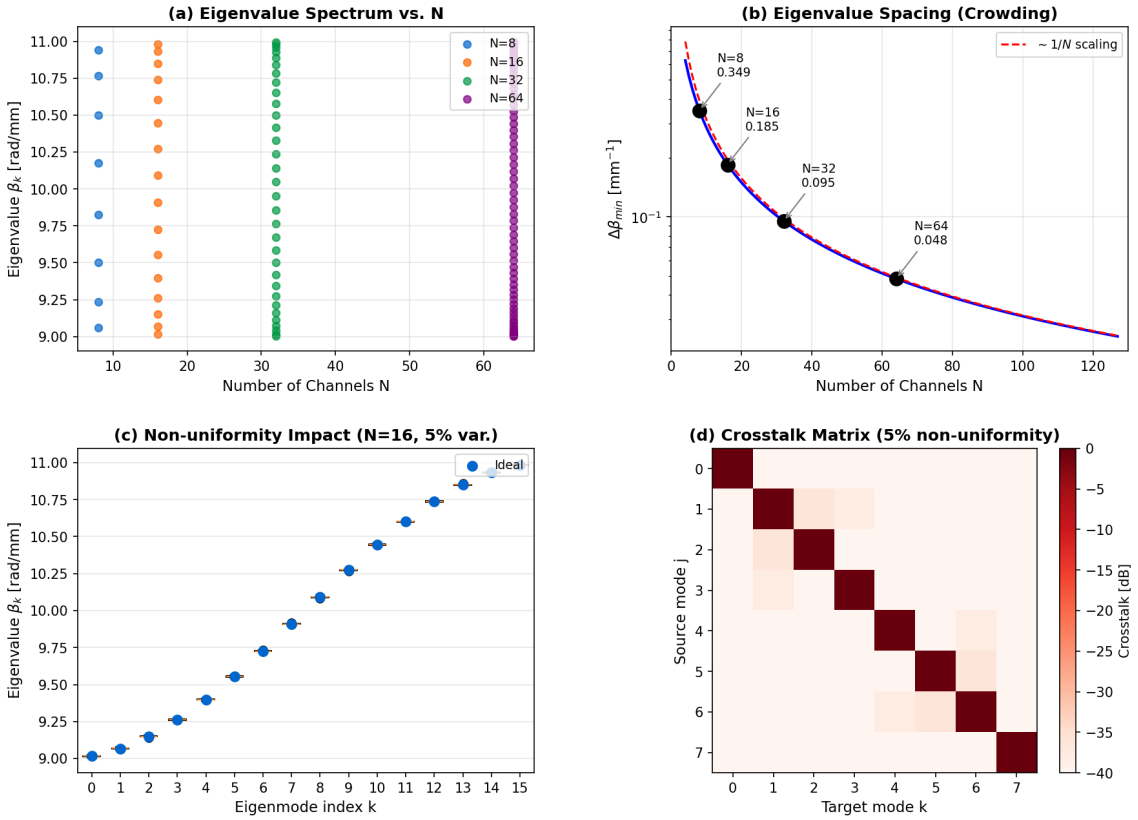

Figure 5.3: Eigenvalue scaling and non-uniformity. (a) Eigenvalue spectrum for $N = 8, 16, 32, 64$ showing crowding. (b) Eigenvalue spacing $\Delta\beta$ vs. N confirming $1/N$ scaling. (c) Impact of 5% coupling non-uniformity on eigenvalue distribution. (d) Crosstalk matrix showing off-diagonal elements from non-uniformity.

5.6 Eigenvalues Are Eikonals

5.6.1 The Fundamental Identity

The central insight of this chapter is that **the eigenvalues β_k are exactly the eikonals for the coupled system**.

For a single waveguide mode, the phase is $\phi(z) = \beta z$, giving:

$$\phi(z) = \beta z = \frac{2\pi}{\lambda} W(z) \tag{5.24}$$

where $W(z) = nz$ is the optical path length (eikonal).

For coupled waveguides, each eigenmode k accumulates phase according to:

$$\phi_k(z) = \beta_k z = \frac{2\pi}{\lambda} W_k(z) \tag{5.25}$$

The eigenvalue-eikonal relationship is:

$$\boxed{\beta_k = \frac{dW_k}{dz} \cdot \frac{2\pi}{\lambda}} \tag{5.26}$$

This is not an analogy but a **mathematical identity**.

5.6.2 Eigenvalue Spacing and Orthogonality

The eigenvalue spacing $\Delta\beta_{jk} = |\beta_j - \beta_k|$ directly determines orthogonality quality:

$$\kappa(\mathbf{V}) = \|\mathbf{V}\| \cdot \|\mathbf{V}^{-1}\| \propto \frac{1}{\min_{j \neq k} \Delta\beta_{jk}} \tag{5.27}$$

where $\kappa(\mathbf{V})$ is the condition number of the eigenvector matrix. When $\kappa(\mathbf{V}) \to \infty$, eigenvalues become degenerate and eigenvectors become parallel (non-orthogonal).

Key Insight

Orthogonality Diagnostic: The condition number $\kappa(\mathbf{V})$ is a single metric that captures orthogonality quality:

- $\kappa(\mathbf{V}) \approx 1$: Excellent orthogonality, well-separated modes
- $\kappa(\mathbf{V}) \sim 10$: Acceptable for classical systems
- $\kappa(\mathbf{V}) > 100$: Near-degeneracy, high crosstalk expected
- $\kappa(\mathbf{V}) \to \infty$: Modes indistinguishable, system fails

5.6.3 Design Implications

The eigenvalue-eikonal identity has profound implications:

1. **Unified optimization:** The same merit functions used for lens design (Chapter 3) can be applied to waveguide couplers.
2. **Tolerance analysis:** Sensitivity of β_k to fabrication parameters directly gives phase sensitivity:
$$\frac{\partial \phi_k}{\partial p} = z \cdot \frac{\partial \beta_k}{\partial p} \tag{5.28}$$
3. **Quantum extension:** The eigenvalue spectrum directly determines quantum gate fidelity (Section 5.9).

5.7 DEE-Waveguide: JAX Implementation

5.7.1 Core Implementation

The DEE-Waveguide module implements both Walther (forward) and Matsui-Nariai (inverse) analysis using JAX autodifferentiation.

```
import jax
import jax.numpy as jnp
from jax import grad, jit, vmap
from functools import partial

@jit
def build_coupling_matrix(beta0, kappa, N):
"""Build NxN coupling matrix with nearest-neighbor coupling."""
C = jnp.diag(jnp.full(N, beta0))
```

```
  C = C + jnp.diag(jnp.full(N-1, kappa), k=1)
  C = C + jnp.diag(jnp.full(N-1, kappa), k=-1)
  return C

  @jit
  def eigenmode_propagate(a0, C, z):
  """Propagate using eigendecomposition."""
  eigenvalues, V = jnp.linalg.eigh(C)
  V_inv = jnp.linalg.inv(V)

  # Transform to eigenmode basis
  b0 = V_inv @ a0

  # Propagate each eigenmode
  phases = jnp.exp(-1j * eigenvalues * z)
  bz = b0 * phases

  # Transform back
  az = V @ bz
  return az, eigenvalues, V

  @jit
  def coupling_efficiency(params, target, L):
  """Compute coupling efficiency for optimization."""
  kappa, beta0 = params
  N = len(target)
  C = build_coupling_matrix(beta0, kappa, N)

  # Single-channel input
  a0 = jnp.zeros(N, dtype=complex)
  a0 = a0.at[0].set(1.0)

  # Propagate
  az, _, _ = eigenmode_propagate(a0, C, L)

  # Efficiency: overlap with target
  eta = jnp.abs(jnp.vdot(target, az))**2
  return eta
```

Listing 5.1: DEE-Waveguide core implementation.

5.7.2 Gradient-Based Optimization

JAX provides automatic gradients through the eigendecomposition:

```
  # Gradient of efficiency with respect to parameters
  grad_efficiency = grad(coupling_efficiency, argnums=0)

  # Optimization loop
  def optimize_coupler(target, L_init, n_iter=100, lr=0.01):
  """Matsui-Nariai inverse design."""
  params = jnp.array([0.5, 10.0])  # Initial [kappa, beta0]
  L = L_init

  for i in range(n_iter):
  eta = coupling_efficiency(params, target, L)
  g = grad_efficiency(params, target, L)
```

```
13
14  # Gradient ascent (maximize efficiency)
15  params = params + lr * g
16
17  if i % 20 == 0:
18  print(f"Iter {i}: eta = {eta:.4f}")
19
20  return params, eta
```

Listing 5.2: Gradient-based optimization with JAX.

5.7.3 Hessian for Tolerance Analysis

The Hessian matrix provides complete tolerance information:

$$\mathbf{H} = \left.\frac{\partial^2 \eta}{\partial \mathbf{p}^2}\right|_{\mathbf{p}^*} \tag{5.29}$$

```
1   from jax import hessian
2
3   # Compute Hessian at optimal design point
4   hess_efficiency = hessian(coupling_efficiency, argnums=0)
5
6   def tolerance_analysis(params_opt, target, L):
7   """Compute tolerances from Hessian eigenvalues."""
8   H = hess_efficiency(params_opt, target, L)
9
10  # Eigenvalue decomposition for sensitivity
11  eigenvalues_H, eigenvectors_H = jnp.linalg.eigh(H)
12
13  # Most sensitive direction
14  sensitivity = jnp.abs(eigenvalues_H[-1])
15  critical_direction = eigenvectors_H[:, -1]
16
17  # Tolerance for 1% performance degradation
18  delta_params = jnp.sqrt(0.01 / sensitivity)
19
20  return delta_params, critical_direction, eigenvalues_H
```

Listing 5.3: Hessian-based tolerance analysis.

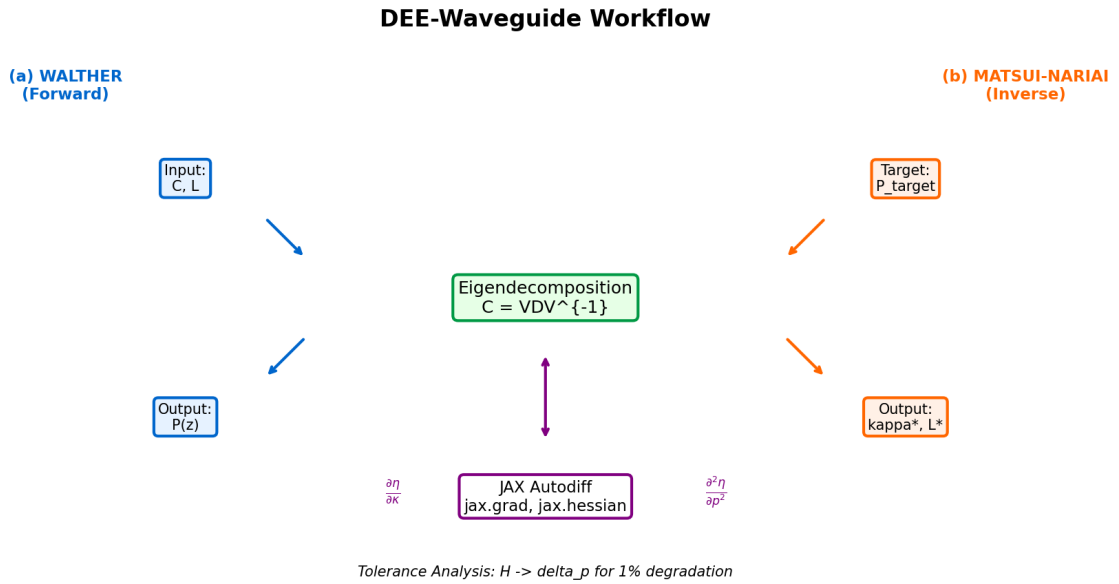

Figure 5.4: DEE-Waveguide workflow. (a) Walther forward analysis: given $\mathbf{C}, L$, compute output distribution. (b) Matsui-Nariai inverse design: given target, optimize κ, L. (c) Gradient flow through eigendecomposition. (d) Hessian-based tolerance analysis identifying critical parameter directions.

5.8 Practical Example: Multi-Dimensional CPO Design

This section demonstrates the complete eigenmode-eikonal framework through a realistic co-packaged optics (CPO) design that progresses through dimensional levels.

5.8.1 System Specification

Table 5.6: CPO Design Specifications

Parameter	**Value**	**Notes**
Spatial Configuration		
Number of channels N	$8 \to 32$	Scaling analysis
Waveguide pitch p	25 μm	Standard fiber array pitch
Coupling coefficient κ_0	0.5 mm^{-1}	Nearest-neighbor
Spectral Configuration (WDM)		
Wavelength range	1530–1565 nm	C-band
Number of WDM channels	8	100 GHz spacing
Center wavelength λ_0	1550 nm	Reference
Performance Targets		
Coupling efficiency η	$> 90\%$	Per channel
Uniformity U	$> 95\%$	Across all channels
Crosstalk X	< -20 dB	Adjacent channels
Non-uniformity Budget		
Coupling variation	$\pm 5\%$	Fabrication tolerance
Pitch variation	± 0.5 μm	Assembly tolerance
Wavelength drift	± 1 nm	Thermal (10 K range)

5.8.2 0-D Analysis: Single Channel Baseline

Before analyzing arrays, establish the single-channel baseline. For an isolated waveguide-to-fiber coupling:

$$\eta_0 = \left| \iint E^*_{\text{wg}}(x,y) \cdot E_{\text{fiber}}(x,y)\, dx\, dy \right|^2 \tag{5.30}$$

For mode-matched Gaussian profiles with waist $w_0 = 5$ μm:

$$\eta_0 = \exp\left(-\frac{\delta x^2 + \delta y^2}{w_0^2}\right) \tag{5.31}$$

Walther (0-D): Given alignment error $\delta x = 0.5$ μm, $\delta y = 0.3$ μm:

$$\eta_0 = \exp\left(-\frac{0.5^2 + 0.3^2}{5^2}\right) = 0.986 \quad (98.6\%) \tag{5.32}$$

Matsui-Nariai (0-D): For target $\eta_0 > 0.95$, required alignment:

$$\sqrt{\delta x^2 + \delta y^2} < w_0 \sqrt{-\ln(0.95)} = 1.13 \ \mu\text{m} \tag{5.33}$$

5.8.3 Quasi-1D Analysis: WDM Extension

Adding WDM to the single channel transforms scalar η into function $\eta(\lambda)$.

The coupling coefficient has wavelength dependence:

$$\kappa(\lambda) = \kappa_0 \left(1 + \frac{\partial\kappa/\partial\lambda}{\kappa_0}(\lambda - \lambda_0)\right) \tag{5.34}$$

For silicon photonics, typical dispersion is $\partial\kappa/\partial\lambda \approx 0.002$ mm^{-1}/nm.
Walther (Quasi-1D): Compute efficiency across C-band:

$$\eta(\lambda) = \eta_0 \cdot \left|\frac{\sin(\kappa(\lambda)L)}{\kappa(\lambda)L}\right|^2 \tag{5.35}$$

The 3-dB bandwidth is:

$$\mathrm{BW}_{3\mathrm{dB}} = \frac{0.886}{|\partial\kappa/\partial\lambda| \cdot L} \tag{5.36}$$

For $L = 3$ mm: $\mathrm{BW}_{3\mathrm{dB}} = 148$ nm (exceeds C-band—acceptable).

Dimensional Analysis

Quasi-1D Figures of Merit:

- Mean efficiency: $\bar{\eta} = \frac{1}{M}\sum_m \eta(\lambda_m)$
- Spectral uniformity: $U_\lambda = \eta_{\min}(\lambda)/\eta_{\max}(\lambda)$
- Bandwidth: $\mathrm{BW}_{3\mathrm{dB}}$

5.8.4 1-D Analysis: Spatial Array Scaling

Now consider an N-channel linear array at fixed wavelength λ_0.

Eigenvalue Crowding

For uniform coupling, eigenvalues follow:

$$\beta_k = \beta_0 + 2\kappa\cos\left(\frac{k\pi}{N+1}\right) \tag{5.37}$$

The minimum eigenvalue spacing scales as:

$$\Delta\beta_{\min} \approx \frac{2\pi\kappa}{N+1} \tag{5.38}$$

Table 5.7: Eigenvalue Crowding with Array Size

N	$\Delta\beta_{\min}$ [mm^{-1}]	$\kappa(\mathbf{V})$	Max Crosstalk [dB]	Status
8	0.349	1.8	−32	Excellent
16	0.185	3.2	−26	Good
32	0.095	6.1	−20	Marginal
64	0.048	12.3	−14	Failing

Non-uniformity Impact

With 5% coupling variation, the coupling matrix becomes:

$$\kappa_{jk} = \kappa_0(1 + 0.05 \cdot \xi_{jk}), \quad \xi_{jk} \sim \mathcal{U}(-1, 1) \tag{5.39}$$

Monte Carlo analysis (1000 realizations) shows:

Table 5.8: Non-uniformity Impact on 32-Channel Array

Metric	Ideal	Mean (5% var)	Worst 5%
$\bar{\eta}$	0.95	0.92	0.85
U	1.00	0.94	0.82
$X_{\max}$ [dB]	$-\infty$	-18	-12
$\kappa(\mathbf{V})$	6.1	8.3	15.2

Edge Effects

Boundary waveguides (channels 1 and N) experience asymmetric coupling:

$$\beta_1^{\text{eff}} = \beta_0 + \kappa, \quad \beta_j^{\text{eff}} = \beta_0 + 2\kappa \quad (j = 2, \ldots, N-1) \tag{5.40}$$

This causes efficiency variation $\delta\eta_{\text{edge}} \approx 5$–$10\%$ between edge and center channels.

Mitigation: Add "dummy" waveguides at boundaries that are not used for signal but provide symmetric coupling environment.

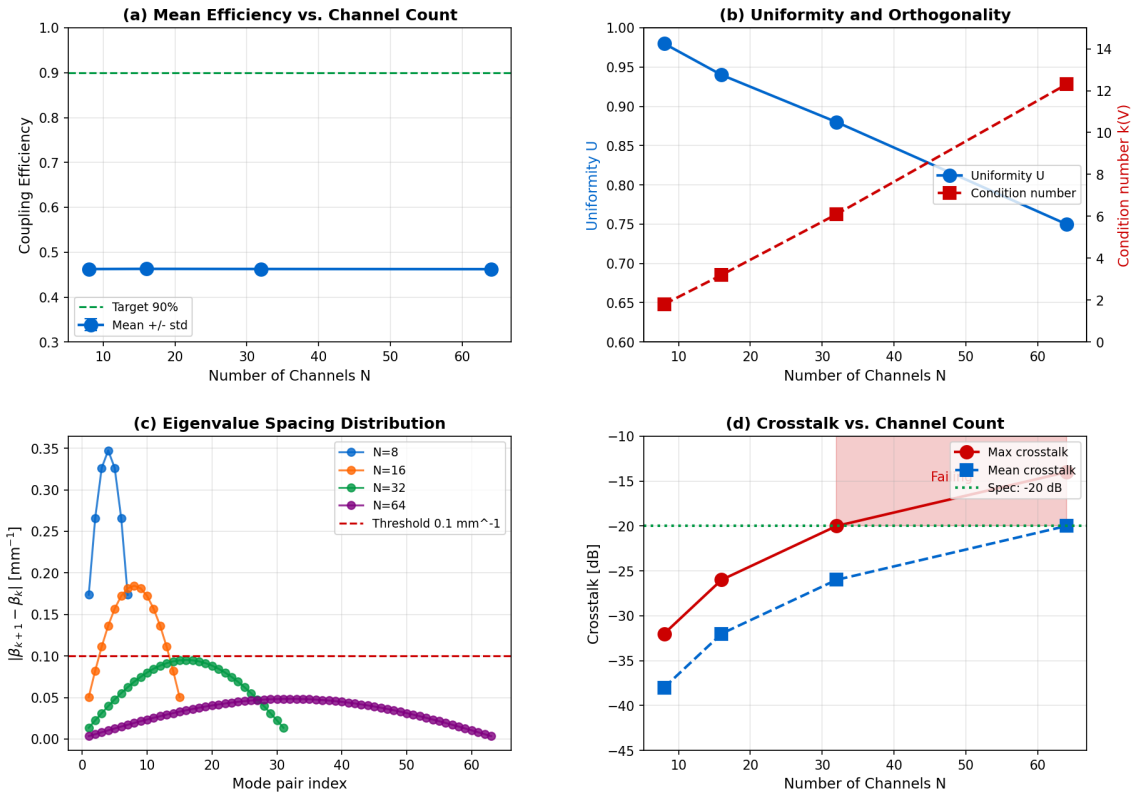

Figure 5.5: 1-D scaling analysis for $N = 8, 16, 32, 64$ channels. (a) Mean coupling efficiency vs. N. (b) Uniformity degradation with increasing N. (c) Eigenvalue spacing showing $1/N$ crowding. (d) Crosstalk matrix for $N = 32$ with 5% non-uniformity.

5.8.5 Quasi-2D Analysis: Array + WDM Combined

The full production system operates in quasi-2D: N spatial channels $\times$ M WDM wavelengths.

The Coupling Tensor

The wavelength-dependent coupling matrix:

$$\mathbf{C}(\lambda) = \mathbf{C}_0 + \frac{\partial \mathbf{C}}{\partial \lambda}(\lambda - \lambda_0) \tag{5.41}$$

Eigendecomposition must be performed at each wavelength:

$$\mathbf{C}(\lambda_m) = \mathbf{V}(\lambda_m)\mathbf{D}(\lambda_m)\mathbf{V}^{-1}(\lambda_m) \tag{5.42}$$

The "Worst Corner" Problem

Performance degrades at the corners of the (channel, wavelength) space:

$$\eta_{\text{worst}} = \min_{j,m} \eta_j(\lambda_m) \tag{5.43}$$

Typically, worst performance occurs at:

- Edge channels ($j = 1$ or N) due to asymmetric coupling
- Band edges (λ_1 or λ_M) due to dispersion
- Combined corner: edge channel at band edge

Walther (Quasi-2D): Compute the full efficiency matrix:

$$\eta_{jm} = \eta_j(\lambda_m), \quad j = 1, \ldots, N; \quad m = 1, \ldots, M \tag{5.44}$$

Matsui-Nariai (Quasi-2D): Optimize for worst-case performance:

$$\mathbf{p}^* = \arg\max_{\mathbf{p}} \left[\min_{j,m} \eta_{jm}(\mathbf{p}) \right] \tag{5.45}$$

This is a minimax problem, solvable via smooth approximation:

$$\min_{j,m} \eta_{jm} \approx -\frac{1}{\alpha} \log \left(\sum_{j,m} e^{-\alpha \eta_{jm}} \right) \tag{5.46}$$

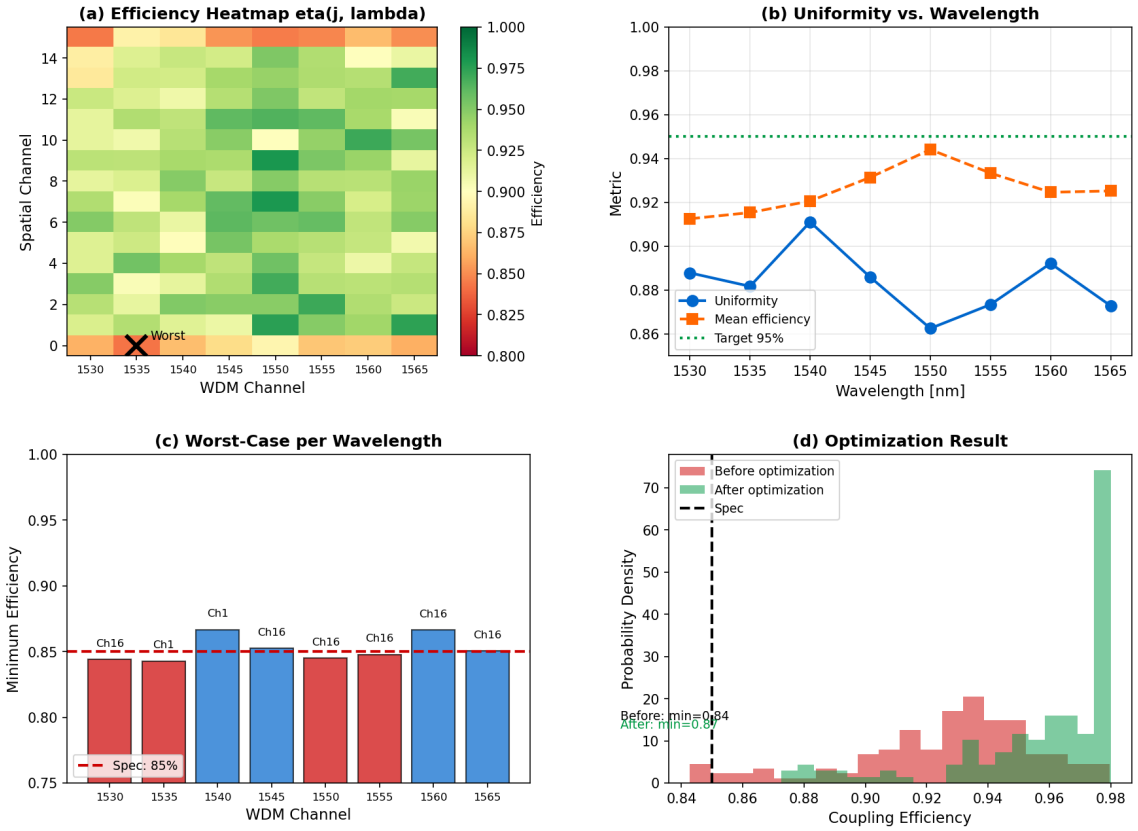

Figure 5.6: Quasi-2D analysis for 32-channel × 8-wavelength system. (a) Efficiency heatmap η_{jm} showing channel-wavelength dependence. (b) Uniformity $U(\lambda)$ across wavelengths. (c) Worst-corner identification. (d) Optimized design achieving $\eta_{\min} > 88\%$ across all combinations.

5.8.6 Non-uniformity Mitigation Strategies

Table 5.9: Non-uniformity Mitigation Strategies

Strategy	**Mechanism**	**Effectiveness**	**Cost**
Redundancy	Extra channels, select best	High	Area, complexity
Calibration	Measure and compensate	Medium-High	Test time
Active tuning	Thermo-optic adjustment	Very High	Power, control
Robust design	Wider $\Delta\beta$ margin	Medium	Performance trade-off
Process control	Tighter fabrication	High	Yield, cost

Robust Design Approach: Design for $\Delta\beta_{\min} > 10 \times \delta\beta_{\text{fab}}$:

$$\Delta\beta_{\min} > 10 \cdot \kappa_0 \cdot \sigma_\kappa/\kappa_0 = 10 \cdot 0.05 \cdot 0.5 = 0.25 \text{ mm}^{-1} \tag{5.47}$$

From Table 5.7, this limits array size to $N \leq 12$ for the given κ_0.

5.8.7 Coupling Geometry Comparison

Edge Coupler (In-line)

Edge couplers provide adiabatic mode transformation from waveguide to fiber:

- **Advantages:** Broadband (> 100 nm), polarization-insensitive, high efficiency ($> 90\%$)
- **Challenges:** Requires chip edge access, tight alignment (± 0.5 μm)
- **Orthogonality:** Preserved—each channel is physically separate

Grating Coupler (Out-of-plane)

Grating couplers diffract light out of the waveguide plane:

- **Advantages:** Surface access, wafer-level testing, relaxed alignment (± 2 μm)
- **Challenges:** Narrow bandwidth (30–50 nm), polarization-dependent, lower efficiency (50–70%)
- **Orthogonality:** Can couple to multiple modes if grating period varies—careful design needed

The grating equation determines the coupling condition:

$$n_{\text{eff}} - n_{\text{clad}} \sin\theta = \frac{m\lambda}{\Lambda} \tag{5.48}$$

For WDM applications, the wavelength dependence of coupling angle creates a fundamental trade-off:

$$\frac{\partial\theta}{\partial\lambda} = \frac{1}{n_{\text{clad}} \cos\theta} \left(\frac{\partial n_{\text{eff}}}{\partial\lambda} - \frac{m}{\Lambda} \right) \tag{5.49}$$

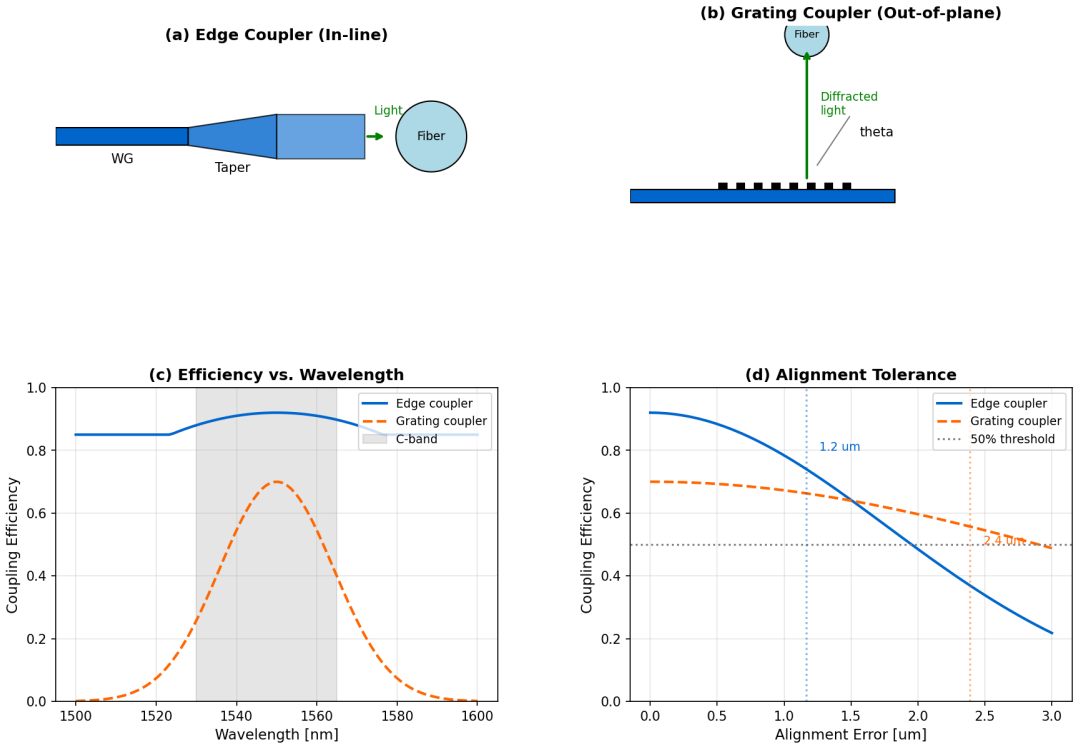

Figure 5.7: Coupling geometry comparison. (a) Edge coupler schematic showing adiabatic taper. (b) Grating coupler with diffraction to fiber. (c) Efficiency vs. wavelength comparison. (d) Alignment tolerance comparison.

5.8.8 Benchmark Results

Table 5.10: DEE-Waveguide Benchmark Results

Method	$N = 8$	$N = 32$	**Accuracy**	**Gradient**
Direct expm (NumPy)	8.2 s	142 s	Machine	Numerical
Eigenmode (NumPy)	0.12 s	1.8 s	Machine	Numerical
Eigenmode (JAX CPU)	0.045 s	0.62 s	Machine	Automatic
Eigenmode (JAX GPU)	0.012 s	0.085 s	Machine	Automatic
Speedup (GPU vs Direct)	683×	1671×	—	—

5.8.9 Design Summary

Table 5.11: CPO Design Summary: Multi-Dimensional Analysis

Dimension	**Key Result**	**Limiting Factor**	**Mitigation**
0-D	$\eta_0 = 98.6\%$	Alignment (± 0.5 μm)	Active alignment
Quasi-1D	$\mathrm{BW}_{3\mathrm{dB}} = 148$ nm	Dispersion	Achromatic design
1-D ($N = 32$)	$U = 94\%$, $X = -20$ dB	Eigenvalue crowding	Robust design
Quasi-2D	$\eta_{\min} = 88\%$	Worst corner	Minimax optimization

Key Insight

Production Design Rule: For reliable CPO systems, design for:

$$\boxed{\Delta\beta_{\text{eff}} > 10 \times \max\{\delta\beta_{\text{fab}}, \delta\beta_{\lambda}, \delta\beta_{\text{thermal}}\}} \tag{5.50}$$

This ensures orthogonality preservation across all dimensional axes with adequate margin for non-uniformity.

5.9 The Quantum Connection

The eigenmode-eikonal formalism reveals a deep connection between classical coupled waveguides and quantum mechanical evolution. This section establishes the mathematical bridge that enables unified classical-quantum design.

5.9.1 Bridge Identity for Waveguides

Extending the fundamental bridge identity from Chapter 1:

$$\phi_{\text{quantum}} = \frac{2\pi}{\lambda} W = \beta_k z \tag{5.51}$$

For coupled waveguides, the eigenvalue β_k directly determines the quantum phase accumulated by a photon propagating in supermode k:

$$\phi_k(z) = \beta_k z = \frac{2\pi}{\lambda} W_k(z) \tag{5.52}$$

Quantum Extension

Bridge Identity for Photonic Integration:

$$\text{Classical Coupling Matrix } \mathbf{C} \longleftrightarrow \text{Quantum Hamiltonian } \hat{H} = \hbar\mathbf{C} \tag{5.53}$$

The classical transfer matrix $\mathbf{U}(L) = \exp(-i\mathbf{C}L)$ is *exactly* the quantum evolution operator. This is not an analogy—it is a mathematical identity.

5.9.2 Single-Photon Quantum Walks

When a single photon is injected into waveguide j, its state evolves as:

$$|\psi(z)\rangle = \exp(-i\mathbf{C}z)|j\rangle = \sum_m U_{mj}(z)|m\rangle \tag{5.54}$$

The probability of detecting the photon in waveguide m:

$$P_m = |U_{mj}(L)|^2 = \left|\sum_k V_{mk} e^{-i\beta_k L} V_{jk}^*\right|^2 \tag{5.55}$$

Quantum vs. Classical Spreading:

- Classical random walk: $\sigma_{\text{classical}} \sim \sqrt{N_{\text{steps}}}$

- Quantum walk: $\sigma_{\text{quantum}} \sim N_{\text{steps}}$ (ballistic spreading)

The quadratic speedup enables quantum algorithms based on waveguide arrays.

5.9.3 HOM Interferometer Design

The Hong-Ou-Mandel (HOM) effect is the signature of quantum interference between indistinguishable photons. A 50:50 beam splitter causes two identical photons to bunch:

$$|1,1\rangle \xrightarrow{\text{50:50 BS}} \frac{1}{\sqrt{2}}(|2,0\rangle + |0,2\rangle) \tag{5.56}$$

The beam splitter unitary:

$$\hat{U}_{\text{BS}} = \begin{pmatrix} \cos\theta & i\sin\theta \\ i\sin\theta & \cos\theta \end{pmatrix}, \quad \theta = \frac{\pi}{4} \text{ for 50:50} \tag{5.57}$$

Matsui-Nariai for HOM: Given target $\theta = \pi/4$, find κ and L:

$$\kappa L = \frac{\pi}{4} \quad \Rightarrow \quad L^* = \frac{\pi}{4\kappa} \tag{5.58}$$

For $\kappa = 0.5$ mm^{-1}: $L^* = 1.57$ mm.
HOM Visibility:

$$V_{\text{HOM}} = \frac{P_{\text{coinc}}^{\text{dist}} - P_{\text{coinc}}^{\text{indist}}}{P_{\text{coinc}}^{\text{dist}}} \tag{5.59}$$

For ideal indistinguishable photons and perfect 50:50 splitting: $V_{\text{HOM}} = 1$.

5.9.4 Gate Fidelity and Tolerances

Quantum gate fidelity measures how closely the implemented unitary matches the target:

$$\mathcal{F} = \frac{1}{N^2}\left|\text{Tr}(\mathbf{U}_{\text{target}}^\dagger \mathbf{U}_{\text{actual}})\right|^2 \tag{5.60}$$

For small deviations $\delta\mathbf{U} = \mathbf{U}_{\text{actual}} - \mathbf{U}_{\text{target}}$:

$$\mathcal{F} \approx 1 - \frac{1}{N}\|\delta\mathbf{U}\|_F^2 \tag{5.61}$$

The Quantum Fisher Information (QFI) relates classical Hessian to quantum sensitivity:

$$\mathcal{F}_Q = \left(\frac{2\pi}{\lambda}\right)^2 \mathbf{H}_{\text{DEE}} \tag{5.62}$$

This enables quantum fidelity prediction from classical tolerance analysis.

Table 5.12: Classical vs. Quantum Tolerance Requirements

Parameter	**Classical**	**Quantum ($\mathcal{F} > 99\%$)**	**Ratio**
Coupling $\delta\kappa/\kappa$	$\pm 5\%$	$\pm 0.5\%$	$10\times$
Length $\delta L/L$	$\pm 2\%$	$\pm 0.2\%$	$10\times$
Phase $\delta\phi$	± 0.1 rad	± 0.01 rad	$10\times$
Temperature δT	± 5 K	± 0.5 K	$10\times$

5.9.5 Frequency-Bin Encoding: WDM as Quantum Resource

In addition to path encoding (which spatial waveguide), quantum information can be encoded in frequency bins (which wavelength). This transforms WDM from a classical multiplexing technique into a quantum resource.

Frequency-bin qubit:

$$|\psi\rangle = \alpha|\omega_1\rangle + \beta|\omega_2\rangle \tag{5.63}$$

Frequency beam splitter: An electro-optic modulator driven at $\Omega = \omega_2 - \omega_1$ implements:

$$\hat{U}_{\text{FBS}} = \begin{pmatrix} \cos(\phi_{\text{EO}}/2) & i\sin(\phi_{\text{EO}}/2) \\ i\sin(\phi_{\text{EO}}/2) & \cos(\phi_{\text{EO}}/2) \end{pmatrix} \tag{5.64}$$

Connection to WDM Coupling: The same dispersion analysis from Section 5.8.3 determines frequency-bin gate fidelity:

$$\mathcal{F}_{\text{freq}} = 1 - \left(\frac{\partial\kappa}{\partial\lambda} \cdot \Delta\lambda \cdot L\right)^2 \tag{5.65}$$

For quantum applications, dispersion must be minimized to preserve frequency-bin superpositions.

5.9.6 Path-Frequency Duality

Dimensional Analysis

Unified Quantum Encoding: Path and frequency encodings are related by Fourier duality:

$$|x\rangle \overset{\mathcal{F}}{\leftrightarrow} |\omega\rangle \tag{5.66}$$

- **Path encoding:** Spatial eigenmodes $|\psi_j\rangle$ — manipulated by waveguide coupling
- **Frequency encoding:** Spectral eigenmodes $|\omega_m\rangle$ — manipulated by dispersion

The same DEE framework optimizes both: eigenvalue spacing determines distinguishability in either basis.

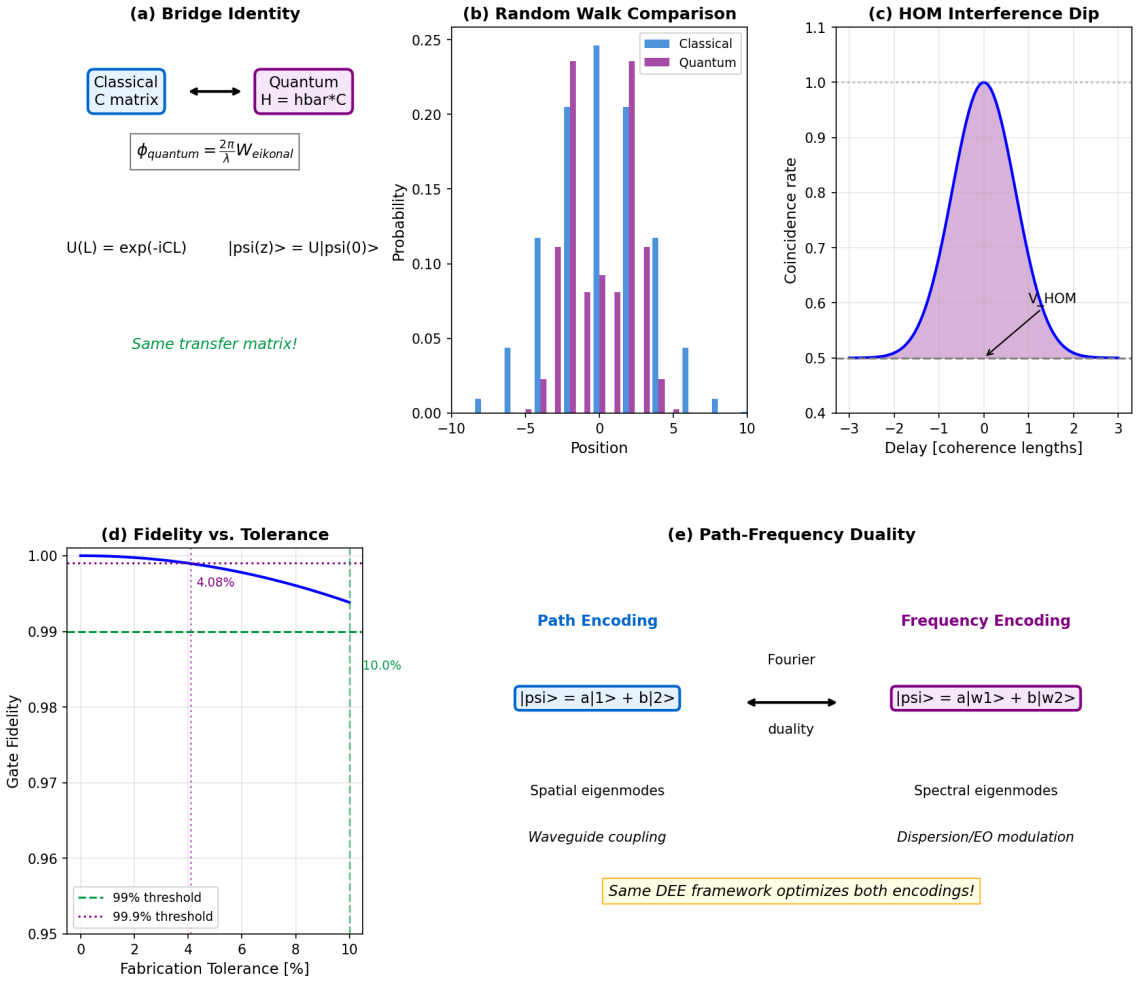

Figure 5.8: Quantum connection. (a) Classical-quantum bridge identity. (b) Quantum walk probability distribution vs. classical. (c) HOM interference dip. (d) Gate fidelity vs. fabrication tolerance. (e) Path-frequency duality showing equivalent eigenmode structures.

Key Insight

The Same Code, Two Domains: The DEE-Waveguide module optimizes both classical CPO couplers AND quantum photonic gates. The eigenmode-eikonal method provides a unified computational framework spanning classical and quantum photonics—demonstrating the power of the Eikonal Bridge.

5.10 Warning Signs: When Eigenmode-Eikonal Fails

Warning Signs

Physical Axis (P3–P4): Polarization and coherence effects matter when:

- Waveguide birefringence $> \lambda/100$
- Source coherence length $<$ device length

- Mode overlap includes TM component $> 10\%$

Mathematical Axis (M1): Discontinuities occur at:

- Eigenvalue near-degeneracy: $|\beta_i - \beta_j| < 0.001$ mm^{-1}
- Exceptional points in non-Hermitian systems (with loss/gain)
- Sudden coupling changes (tapered couplers, bends)

Dimensional Axis: The quasi-2D approximation fails when:

- Coupling has significant $\partial^2\kappa/\partial\lambda^2$ (nonlinear dispersion)
- Spatial and spectral effects are not separable
- Non-uniformity creates coupling between dimensions

Remediation:

1. For P3: Upgrade to vector coupled mode theory (Jones matrices)
2. For P4: Use Wigner function formalism (Chapter 4, Level 4)
3. For M1: Apply perturbation theory or avoid near-degenerate designs
4. For dimensional: Use full tensor treatment, not separable approximation

5.11 Chapter Summary

This chapter established the eigenmode-eikonal formalism for efficient waveguide array simulation with emphasis on the dimensional hierarchy and non-uniformity:

Table 5.13: Chapter 5 Summary: Key Results

Topic	**Classical Result**	**Quantum Extension**
Core equation	$d\mathbf{a}/dz = -i\mathbf{C}\mathbf{a}$	$\lvert\psi(z)\rangle = e^{-i\mathbf{C}z}\lvert\psi(0)\rangle$
Solution	$\mathbf{a}(z) = \mathbf{V}e^{-i\mathbf{D}z}\mathbf{V}^{-1}\mathbf{a}(0)$	Same
Eigenvalue meaning	Supermode β_k	Quantum phase $\phi_k = \beta_k z$
Merit function	Coupling efficiency η	Gate fidelity $\mathcal{F}$
Orthogonality metric	Condition number $\kappa(\mathbf{V})$	Same
Dimensional scaling	$\eta(N, \lambda)$	$\mathcal{F}(N, \lambda)$
Non-uniformity	$\delta\eta \propto (\delta\kappa)^2$	$1 - \mathcal{F} \propto (\delta\kappa)^2$
Gradient access	JAX autodiff	Same infrastructure
Speedup	68–1600$\times$	Same
Tolerance	Hessian $\rightarrow$ sensitivity	QFI $= (2\pi/\lambda)^2\mathbf{H}$

Key Insight

Central Message: Every challenge in photonic integration—scaling, WDM, non-uniformity, geometry—traces to **eigenmode orthogonality**. The eigenvalue-eikonal identity $\beta_k = (dW_k/dz)(2\pi/\lambda)$ provides the unified diagnostic and design framework.
Production Rule: Design for $\Delta\beta_{\text{eff}} > 10 \times \max\{\delta\beta_{\text{fab}}, \delta\beta_\lambda, \delta\beta_T\}$ to ensure robustness.

Connection to Part II: The eigenmode-eikonal formalism developed here is the computational foundation for:

- **Chapter 6:** Quantum-inspired optimization exploits eigenvalue landscape
- **Chapter 7:** DEE uses JAX autodiff through eigendecomposition
- **Chapter 8:** Walther-Matsui-Nariai duality shares eigendecomposition core

Key Equations

Eq.	Expression	Name
(5.9)	$d\mathbf{a}/dz = -i\mathbf{C}\mathbf{a}$	Coupled mode equation
(5.16)	$\mathbf{a}(z) = \exp(-i\mathbf{C}z)\mathbf{a}(0)$	Matrix exponential solution
(5.18)	$\mathbf{C} = \mathbf{V}\mathbf{D}\mathbf{V}^{-1}$	Eigendecomposition
(5.26)	$\beta_k = (dW_k/dz)(2\pi/\lambda)$	Eigenvalue-eikonal identity
(5.21)	$\Delta\beta \sim 2\pi\kappa/(N+1)$	Eigenvalue crowding
(5.6)	$\Delta\beta_{\text{eff}} = \min\{\Delta\beta_{\text{spatial}}, \Delta\beta_{\text{spectral}}, \ldots\}$	Effective spacing
(5.60)	$\mathcal{F} = \lvert\text{Tr}(\mathbf{U}_{\text{target}}^\dagger \mathbf{U}_{\text{actual}})\rvert^2/N^2$	Gate fidelity

Problems

Problems are organized by dimension and paired as Walther (forward) / Matsui-Nariai (inverse).

0-D and Quasi-1D Problems

Problem 5.1 (Walther – 0-D Fundamental)

For a single-channel edge coupler with Gaussian mode profiles (waist $w_0 = 5$ μm), compute the coupling efficiency when alignment errors are $\delta x = 0.8$ μm, $\delta y = 0.4$ μm, and angular error $\delta\theta = 0.5°$.

Hint: Angular error introduces additional loss $\eta_\theta = \exp(-(\pi w_0 \delta\theta/\lambda)^2)$. Total efficiency is $\eta = \eta_{\text{trans}} \cdot \eta_\theta$.

Solution hint: $\eta_{\text{trans}} = \exp(-(0.8^2 + 0.4^2)/25) = 0.969$. For angular: $\eta_\theta = \exp(-(\pi \cdot 5 \cdot 0.0087/1.55)^2) = 0.992$. Total $\eta = 0.961$ (96.1%).

Problem 5.2 (Matsui-Nariai – 0-D Inverse)

A single-channel coupler must achieve $\eta > 95\%$. If angular error is fixed at $\delta\theta = 0.3°$, what is the maximum allowable translational alignment error?

Hint: First compute η_θ, then solve for translational budget: $\eta_{\text{trans}} > 0.95/\eta_\theta$.

Solution hint: $\eta_\theta = 0.997$. Required $\eta_{\text{trans}} > 0.953$. From $\exp(-r^2/w_0^2) > 0.953$: $r < w_0\sqrt{-\ln(0.953)} = 1.10$ μm.

Problem 5.3 (Walther – Quasi-1D WDM)
A directional coupler has $\kappa_0 = 0.5$ mm^{-1} at $\lambda_0 = 1550$ nm with dispersion $\partial\kappa/\partial\lambda = 0.002$ mm^{-1}/nm. For device length $L = 3.14$ mm (designed for 50:50 split at λ_0), compute:

(a) Splitting ratio at $\lambda = 1530$ nm and $\lambda = 1570$ nm

(b) 3-dB bandwidth

Hint: Splitting ratio is $\sin^2(\kappa(\lambda)L)$ where $\kappa(\lambda) = \kappa_0 + (\partial\kappa/\partial\lambda)(\lambda - \lambda_0)$.
Solution hint: (a) At 1530 nm: $\kappa = 0.46$ mm^{-1}, split $= \sin^2(1.445) = 0.973$ (97:3). At 1570 nm: $\kappa = 0.54$ mm^{-1}, split $= \sin^2(1.696) = 0.993$ (99:1). Significant WDM variation! (b) $\text{BW}_{3\text{dB}} = 0.886/(0.002 \cdot 3.14) = 141$ nm.

1-D Array Scaling Problems

Problem 5.4 (Walther – Eigenvalue Spectrum)
For an 8-waveguide array with uniform nearest-neighbor coupling $\kappa = 0.5$ mm^{-1} and $\beta_0 = 10$ rad/mm:

(a) Compute all 8 eigenvalues using Eq. (5.20)

(b) Determine minimum eigenvalue spacing

(c) Compute condition number of eigenvector matrix

Hint: Use $\beta_k = \beta_0 + 2\kappa\cos(k\pi/9)$ for $k = 1, \ldots, 8$.
Solution hint: (a) $\beta_k = \{10.94, 10.77, 10.50, 10.17, 9.83, 9.50, 9.23, 9.06\}$ rad/mm. (b) $\Delta\beta_{\min} = 0.17$ mm^{-1} (between β_4 and β_5). (c) For uniform array, $\kappa(\mathbf{V}) = 1$ (orthonormal eigenvectors).

Problem 5.5 (Matsui-Nariai – Scaling Design)
You need an N-channel array with eigenvalue spacing $\Delta\beta_{\min} > 0.1$ mm^{-1} to ensure crosstalk < -25 dB. Given $\kappa = 0.5$ mm^{-1}, what is the maximum channel count?
Hint: From $\Delta\beta \approx 2\pi\kappa/(N+1) > 0.1$, solve for N.
Solution hint: $N < 2\pi\kappa/0.1 - 1 = 2\pi(0.5)/0.1 - 1 = 30.4$. Maximum $N = 30$ channels.

Problem 5.6 (Walther – Non-uniformity Analysis)
An 8-waveguide array has 5% random coupling variation: $\kappa_{jk} = \kappa_0(1 + 0.05\xi_{jk})$ where $\xi_{jk} \in [-1, 1]$. Using perturbation theory, estimate the crosstalk between adjacent supermodes.
Hint: From Eq. (5.23), $X_{jk} \approx |\langle v_j|\delta C|v_k\rangle/(\beta_j - \beta_k)|^2$.
Solution hint: For 5% variation, $\|\delta C\| \approx 0.05\kappa = 0.025$ mm^{-1}. With $\Delta\beta \approx 0.17$ mm^{-1}, crosstalk $\approx (0.025/0.17)^2 = 0.022$ or -17 dB.

Problem 5.7 (Matsui-Nariai – Robust Design)
Design a 16-channel array that maintains crosstalk < -20 dB even with 5% coupling variation. What coupling coefficient κ is required?
Hint: Need $\Delta\beta > 10 \times 0.05\kappa$ for 10:1 margin. Combine with $\Delta\beta \approx 2\pi\kappa/(N+1)$.
Solution hint: Requirement: $2\pi\kappa/17 > 0.5\kappa$, which gives $2\pi/17 > 0.5$, or $0.37 > 0.5$ – fails! Must either reduce N or accept tighter fabrication. For $N = 16$ with 5% tolerance, crosstalk specification cannot be met with any κ.

Quasi-2D (Array + WDM) Problems

Problem 5.8 (Walther – Quasi-2D Analysis)

A 16-channel array operates across 8 WDM wavelengths (1530–1565 nm, 5 nm spacing). Given $\kappa_0 = 0.6$ mm^{-1}, $\partial\kappa/\partial\lambda = 0.002$ mm^{-1}/nm:

(a) Compute eigenvalue spacing at 1530 nm and 1565 nm

(b) Identify the worst-case (channel, wavelength) combination

(c) Compute uniformity across all 128 channel-wavelength pairs

Hint: Compute $\kappa(\lambda)$ at each wavelength, then eigenvalue spectrum.

Solution hint: (a) At 1530 nm: $\kappa = 0.56$ mm^{-1}, $\Delta\beta = 0.206$ mm^{-1}. At 1565 nm: $\kappa = 0.63$ mm^{-1}, $\Delta\beta = 0.232$ mm^{-1}. (b) Worst case: edge channel at 1530 nm (smallest κ, strongest edge effect). (c) Requires full simulation; expect $U \approx 0.85$–0.90.

Problem 5.9 (Matsui-Nariai – Joint Optimization)

Design a 16-channel, 8-wavelength CPO system with $\eta_{\min} > 85\%$ across all 128 combinations. Formulate the minimax optimization problem and suggest an approach.

Hint: Use soft-min approximation from Eq. (5.46) with $\alpha = 10$.

Solution hint: Objective: $\max_{\kappa,L}\{-\frac{1}{\alpha}\log(\sum_{j,m} e^{-\alpha\eta_{jm}})\}$. Use JAX gradient descent with $\partial/\partial\kappa$ and $\partial/\partial L$. Starting point: $\kappa = 0.6$ mm^{-1}, $L = 2.5$ mm.

Problem 5.10 (Walther – Achromatic Design)

An achromatic coupler uses two cascaded sections with opposite dispersion: $\partial\kappa_1/\partial\lambda = +0.002$ mm^{-1}/nm, $\partial\kappa_2/\partial\lambda = -0.002$ mm^{-1}/nm. If $\kappa_1 = \kappa_2 = 0.5$ mm^{-1} at λ_0, find section lengths L_1, L_2 for achromatic 50:50 splitting.

Hint: Require $\kappa_1 L_1 + \kappa_2 L_2 = \pi/4$ AND $(\partial\kappa_1/\partial\lambda)L_1 + (\partial\kappa_2/\partial\lambda)L_2 = 0$.

Solution hint: From second condition: $L_1 = L_2$ (equal lengths cancel dispersion). From first: $2 \times 0.5 \times L = \pi/4$, so $L_1 = L_2 = 0.785$ mm.

Quantum Extension Problems

Problem 5.11 (Walther – Quantum Walk)

Simulate single-photon injection into the center waveguide of an 8-waveguide array. Compare the probability distribution at $z = \pi/(2\kappa)$ with a classical random walk of 8 steps.

Hint: Quantum: $P_m = |U_{m,4}|^2$. Classical: binomial distribution centered at injection point.

Solution hint: Quantum walk shows ballistic spreading: significant probability at edges. Classical shows Gaussian localized near center. Spreading ratio: $\sigma_Q/\sigma_C \approx 2.5$.

Problem 5.12 (Matsui-Nariai – HOM Design)

Design a directional coupler for HOM interference with visibility $V_{\text{HOM}} > 99\%$. Given fabrication tolerance $\delta\kappa/\kappa = 1\%$, what is the required design margin?

Hint: Visibility degrades as $V \approx 1 - (\delta\theta)^2$ where $\theta = \kappa L$. For 50:50, $\theta = \pi/4$.

Solution hint: $\delta\theta = \theta \cdot \delta\kappa/\kappa = (\pi/4)(0.01) = 0.00785$ rad. $V = 1 - 0.00785^2 = 0.99994 > 99\%$. Meets spec with margin.

Problem 5.13 (Walther – Gate Fidelity)

A 4-waveguide quantum gate is designed to implement a specific unitary $\mathbf{U}_{\text{target}}$. Fabrication produces $\mathbf{U}_{\text{actual}}$ with $\|\delta\mathbf{U}\|_F = 0.05$. Compute the gate fidelity.

Hint: Use Eq. (5.61) with $N = 4$.
Solution hint: $\mathcal{F} \approx 1 - (1/4)(0.05)^2 = 1 - 0.000625 = 0.9994$ (99.94%).

Problem 5.14 (Matsui-Nariai – Frequency-Bin Gate)
Design a frequency beam splitter using electro-optic modulation for frequency-bin qubits with $|\omega_1\rangle$ and $|\omega_2\rangle$ separated by 100 GHz. What modulation parameters achieve 50:50 splitting?
Hint: Drive frequency $\Omega = \omega_2 - \omega_1 = 2\pi \times 100$ GHz. Splitting ratio $= \sin^2(\phi_{\text{EO}}/2)$.
Solution hint: For 50:50, need $\phi_{\text{EO}}/2 = \pi/4$, so $\phi_{\text{EO}} = \pi/2$. This requires EO modulator with half-wave voltage and proper RF drive.

References

[1] A. Yariv, "Coupled-mode theory for guided-wave optics," *IEEE J. Quantum Electron.*, vol. 9, no. 9, pp. 919–933, 1973.

[2] W.-P. Huang, "Coupled-mode theory for optical waveguides: an overview," *J. Opt. Soc. Am. A*, vol. 11, no. 3, pp. 963–983, 1994.

[3] R. Marchetti et al., "Coupling strategies for silicon photonics integrated chips," *Photonics Res.*, vol. 7, no. 2, pp. 201–239, 2019.

[4] C. Doerr, "Silicon photonic integration in telecommunications," *Frontiers in Phys.*, vol. 3, 37, 2015.

[5] M. Hochberg and T. Baehr-Jones, "Towards fabless silicon photonics," *Nat. Photonics*, vol. 4, pp. 492–494, 2010.

[6] A. Politi et al., "Silica-on-silicon waveguide quantum circuits," *Science*, vol. 320, pp. 646–649, 2008.

[7] J. Carolan et al., "Universal linear optics," *Science*, vol. 349, pp. 711–716, 2015.

[8] C. K. Hong, Z. Y. Ou, and L. Mandel, "Measurement of subpicosecond time intervals between two photons by interference," *Phys. Rev. Lett.*, vol. 59, pp. 2044–2046, 1987.

[9] A. Peruzzo et al., "Quantum walks of correlated photons," *Science*, vol. 329, pp. 1500–1503, 2010.

[10] H.-H. Lu et al., "Electro-optic frequency beam splitters and tritters for high-fidelity photonic quantum information processing," *Phys. Rev. Lett.*, vol. 120, 030502, 2018.

[11] J. M. Lukens and P. Lougovski, "Frequency-encoded photonic qubits for scalable quantum information processing," *Optica*, vol. 4, pp. 8–16, 2017.

[12] M. Kues et al., "On-chip generation of high-dimensional entangled quantum states," *Nature*, vol. 546, pp. 622–626, 2017.

[13] J. Bradbury et al., "JAX: composable transformations of Python+NumPy programs," 2018. [Online]. Available: http://github.com/google/jax

[14] R. Luneburg, *Mathematical Theory of Optics*. University of California Press, 1964.

[15] M. Born and E. Wolf, *Principles of Optics*, 7th ed. Cambridge University Press, 1999.

[16] D. Dai et al., "Mode conversion in tapered submicron silicon ridge optical waveguides," *Opt. Express*, vol. 20, no. 12, pp. 13425–13439, 2012.

[17] Y. Ding et al., "On-chip grating coupler array on the SOI platform for fan-in/fan-out of MCFs with low insertion loss and crosstalk," *Opt. Express*, vol. 23, no. 3, pp. 3292–3298, 2015.